

## Microstructure of free volume in SMA copolymers II. Local free volume from PALS

D. Kilburn<sup>a,\*</sup>, G. Dlubek<sup>a,b</sup>, J. Pionteck<sup>c</sup>, D. Bamford<sup>a</sup>, M.A. Alam<sup>a</sup>

<sup>a</sup>*H. H. Wills Physics Laboratory, University of Bristol, Tyndall Avenue, Bristol BS8 1TL, UK*

<sup>b</sup>*ITA Institut fuer innovative Technologien GmbH, Koethen, Aussenstelle Halle, Wiesenring 4, D-06120 Lieskau (bei Halle/S), Germany*

<sup>c</sup>*Leibniz-Institut fuer Polymerforschung e.V. Dresden, Hohe Strasse 6, D-01069 Dresden, Germany*

Received 13 July 2004; received in revised form 25 October 2004; accepted 22 November 2004

Available online 8 December 2004

### Abstract

The structure of the free volume and its temperature dependence between, at maximum 133 and 503 K of copolymers of styrene with maleic-anhydride, SMA (0–35 mol% MA), is studied by pressure–volume–temperature (PVT) experiments and positron annihilation lifetime spectroscopy (PALS). In this second part of the work, PALS data are reported from which the temperature dependence of the mean size and size distribution of local free volumes (subnanometer size holes) is analysed. The mean hole volume,  $\nu_h$ , varies in PS between  $80 \text{ \AA}^3$  (133 K) and  $212 \text{ \AA}^3$  (503 K) and shows a systematic decrease with increasing MA content for a given temperature above  $T_g$ . The specific number of holes,  $N_h'$ , estimated from a comparison of PVT and PALS results, increases slightly with MA content from  $N_h' = (0.60 \pm 0.02) \times 10^{21} \text{ g}^{-1}$  to  $N_h' = (0.70 \pm 0.02) \times 10^{21} \text{ g}^{-1}$  which corresponds to  $N_h(T_g) = N_h'/V_g = 0.62\text{--}0.82 \text{ nm}^{-3}$  ( $V_g$  is the material's specific volume at  $T_g$ ) and  $1/N_h(T_g) = 1.6\text{--}1.2 \text{ nm}^3$  for the volume which contains one hole. The analysed size distributions of the holes above  $T_g$  follow the compressibility of the free volume as it is predicted by the theory of thermal volume fluctuation. We also comment on the connection between the hole size as measured by PALS and the size of a cluster of randomly distributed unoccupied cells as defined by the Simha–Somcynsky theory.

© 2004 Elsevier Ltd. All rights reserved.

**Keywords:** Positron annihilation; Glass transition; Copolymers

### 1. Introduction

This paper is the second part of a work, which consists of two papers (see Ref. [1] for paper I). The aim of our research is to characterize the microstructure of the free volume in a series of copolymers of styrene with maleic anhydride, SMA (0–35 mol% MA). We use positron annihilation lifetime spectroscopy (PALS) [2–4], a method which can measure the mean size and size distribution of subnanometre-size local free volume [2–7], and pressure–volume–temperature (PVT) experiments [8]. In the first part of this work [1], we reported on PVT experiments which were analysed using the Simha–Somcynsky equation of state (S–S eos) [9,10], a lattice-hole theory which describes the

structural disorder in an amorphous material by a lattice with a fraction,  $h$ , of unoccupied cells. From this analysis the temperature and pressure dependence of the specific occupied,  $V_{\text{occ}} = (1-h)V$ , and free volume,  $V_f = hV$ , their isobaric thermal expansivities and their isothermal compressibilities have been determined.

In this part of the work, we focus on the results from the PALS experiments. By comparing the results from this method with the free volume as determined via the S–S eos we calculate the number density of free volume holes. To analyse the positron lifetime spectra we used the new routine, called LT, in its latest version 9.0 [11,12]. This is a non-linear least-squares fitting routine which allows both discrete and log-normally distributed annihilation rates  $\lambda = 1/\tau$ . From these distributions, the mean size and the size distribution of free volume holes can be calculated. We will compare the analysed hole size distribution in relation to theoretical models describing the thermal volume

\* Corresponding author. Tel.: +44 117 928 8963; fax: +44 117 928 8735.

E-mail address: [duncan.kilburn@bristol.ac.uk](mailto:duncan.kilburn@bristol.ac.uk) (D. Kilburn).

fluctuation. We will show that there are clear changes in the free volume parameters with the composition of the SMA copolymers.

## 2. Experimental procedure

### 2.1. Samples

The polystyrene (PS) free of any additives was kindly provided by the BASF AG. The poly(styrene-*co*-maleic anhydride)s (SMA) SMA12 and SMA15 are commercial grade products of Arco Chemicals, while the SMA25, SMA31 and SMA35 were kindly supplied by DSM Research. The products were characterized in part I of our work [1], Table 1 shows the composition and the glass transition temperature,  $T_g$ , from differential scanning calorimetry (DSC). The content of the maleic anhydride units in the polymers was calculated from the sequence distribution of the triads, which was determined from the methylene  $^{13}\text{C}$  NMR subspectra [13].

### 2.2. PALS experiments

The PALS measurements were carried out using a fast-fast coincidence system [2–4] with a time resolution of 260 ps and a channel width of 50 ps. Two identical samples of 1.5 mm thickness were sandwiched around a  $1 \times 10^6$  Bq positron source:  $^{22}\text{NaCl}$ , deposited between two 8  $\mu\text{m}$  thick Kapton foils. To prevent sticking of the source to the samples at higher temperatures, each sample was covered with an additional foil of 8  $\mu\text{m}$  thick Kapton. Source corrections and time resolution (a sum of three Gaussians) were determined by measuring a defect-free aluminum reference. The temperature of the samples, placed in a vacuum chamber was varied, at maximum between 133 and 503 K, in steps of 10 K with an uncertainty of  $\pm 1$  K. For some of the samples the heating scan was followed by a

cooling scan in steps of 10 K down to 293 K. Since we observed no hysteresis in the lifetimes, we will not discuss these results.

Each lifetime spectrum contained  $\sim 10^6$  coincidence counts. We initially used the conventional analysis of lifetime spectra which decomposes the lifetime spectrum into three discrete exponentials  $s(t) = \sum(I_i/\tau_i)\exp(-t/\tau_i)$ ,  $\sum I_i = 1$ ,  $i = 1, 2, 3$ . The routine LT9.0 [11,12] in its discrete mode performs a non-linear least-squares fit to determine the (mean or characteristic) lifetimes  $\tau_i$  of the annihilation channels, their intensities  $I_i$ , the time zero of the spectrum and the background count of the spectrum. The three lifetimes are attributed to annihilation of the *para* state of positronium (a bound electron–positron state) (*p*-Ps,  $\tau_1 \sim 160$  ps), free (not Ps) positrons ( $\tau_2 \sim 370$ –450 ps), and the *ortho* state of positronium (*o*-Ps,  $\tau_3 = 1.5$ –4 ns) [2–4]. In vacuum *o*-Ps has a mean lifetime of 142 ns but this is reduced in amorphous polymers to the value quoted by the positron annihilating with an electron other than its bound partner and of opposite spin (pick-off annihilation).

In amorphous polymers, Ps annihilates from within the small local free volumes (holes) that form the (excess) free volume (Anderson localization [14]). It is either formed in these holes or if not, diffuses there with a mean path length of  $\sim 1$  nm [15]. The *o*-Ps lifetime depends on the size of the hole within which it annihilates, via the well known formula relating the pick-off lifetime ( $\tau_3 = \tau_{po}$ ) to the radius of the hole,  $r_h$

$$\tau_{po} = 0.5 \text{ ns} \left[ 1 - \frac{r_h}{r_h + \delta r} + \frac{1}{2\pi} \sin\left(\frac{2\pi r_h}{r_h + \delta r}\right) \right]^{-1} \quad (1)$$

This formula comes from a simple model incorporating quantum mechanical and empirical arguments [16–18]. The factor of 0.5 ns is the inverse of the spin-averaged Ps annihilation rate,  $\delta r = 1.66 \text{ \AA}$  represents the extent of the penetration of the Ps-wavefunction into the walls of the hole [17,18]. Typical *o*-Ps lifetimes in amorphous polymers are in the ns-range, but as we expect a distribution of hole sizes

Table 1  
Parameters of SMA copolymers – see text for explanations

	$\pm$	PS	SMA12	SMA15	SMA25	SMA31	SMA35
Mol% MA		0	11.8	14.5	25.3	30.9	34.7
$T_g^a$ (K)	2	377	391	403	426	439	449
$T_g^b$ (K)	3	372	377	396	431	427	437
$V_{fg}^c$ ( $\text{cm}^3 \text{g}^{-1}$ )	0.002	0.0692	0.0668	0.0735	0.0727	0.0726	0.0744
$h_g^c$	0.002	0.0716	0.0707	0.0792	0.0815	0.0831	0.0867
$\nu_{hg}$ ( $\text{\AA}^3$ )	8	114.9	108.3	117.1	121.9	109	96.7
$e_{hg}$ ( $\text{\AA}^3 \text{K}^{-1}$ )	0.02	0.221	0.154	0.171	0.197	0.082	0.116
$e_{hr}$ ( $\text{\AA}^3 \text{K}^{-1}$ )	0.06	1.021	0.91	0.864	0.861	0.652	0.751
$dV/d\nu_h, T > T_g \times (10^{21} \text{g}^{-1})$	0.04	0.61	0.62	0.69	0.57	0.66	0.65
$dV_i/d\nu_h \times (10^{21} \text{g}^{-1})$	0.04	0.60	0.61	0.64	0.67	0.65	0.70
$V_{f0}$ ( $\text{cm}^3 \text{g}^{-1}$ )	0.002	0.002	−0.004	−0.004	0.004	−0.015	−0.002
$N_{hg}$ ( $\text{nm}^{-3}$ )	0.02	0.62	0.65	0.69	0.75	0.75	0.82

<sup>a</sup> From DSC.

<sup>b</sup> From PALS.

<sup>c</sup> From PVT, Part I [1].

and shapes it seems reasonable to expect a distribution of lifetimes [19,20]. In its distribution mode, LT can allow a user-defined number of the annihilation rates ( $\lambda_i$ ,  $\lambda_i = 1/\tau_i$ ) to follow a log-normal distribution. The fit of these functions to the spectra provides the annihilation parameters  $\tau_i$  and  $I_i$ , as well as the width of the corresponding distribution (standard deviation  $\sigma_i$  of the lifetime  $\tau_i$ ). In the final fits, we assumed that only the *o*-Ps lifetimes are distributed and constrained the first lifetime to its average value of 160 ps [3].

We observed that for PS  $I_3$  showed an almost monotonous increase from 34% at 130 K to  $I_3=44\%$  at 470 K (not shown). The SMA copolymers exhibit similar behavior, but with systematically lower values of  $I_3$  with increasing MA content. In the SMA35 copolymer, for example,  $I_3=17\%$  at 300 K.  $I_3$  mirrors the Ps yield [3], its reductions can be attributed to inhibition of Ps formation by MA comonomer units which are expected to act as scavengers for excess electrons [21,22]. Since  $I_3$  is not solely dependent on free volume [23,24] it is not discussed here.

### 3. Results and discussion

#### 3.1. Local free volume from PALS

The hole volume  $\nu_h$  calculated from  $\tau_3$  via Eq. (1) and  $\nu_h = 4\pi r_h^3/3$  is shown in Fig. 1. For PS the hole volume varies from  $\nu_h = 80 (\pm 2) \text{ \AA}^3$  ( $r_h = 2.67 \text{ \AA}$ ) at 133 K to  $\nu_h = 212 (\pm 2) \text{ \AA}^3$  ( $r_h = 3.69 \text{ \AA}$ ) at 473 K with a distinct increase in the slope around the  $T_g$  of each SMA copolymer. The standard deviation of the hole size distribution,  $\sigma_{\nu_h}$ , varies in a similar way to the mean hole size, increasing (again for PS) from  $25 \text{ \AA}^3$  at 133 K to  $70 \text{ \AA}^3$  at 473 K. Full details of the calculation of  $\sigma_{\nu_h}$  are given later in this paper. At low temperatures, *o*-Ps is trapped in local free volumes within the glassy matrix and  $\tau_3$ , and hence  $\nu_h$ , show the mean size of static holes. The averaging occurs over the hole sizes and shapes. The slight increase of  $\nu_h$  with temperature mirrors

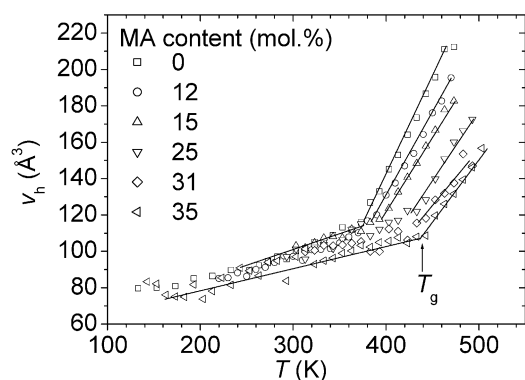


Fig. 1. Mean hole volume  $\nu_h$  (from PALS) vs. temperature,  $T$ , for SMA copolymers.

the thermal expansion of free volume in the glass due to the anharmonicity of molecular vibrations and local motions in the vicinity of the holes. In the rubbery phase,  $T > T_g$ , the molecular and segmental motions increase rapidly resulting in a steep rise in the hole size with temperature. Now  $\nu_h$  represents an average value of the local free volumes whose size and shape fluctuate in space and time, provided the timescale of a typical segmental relaxation is greater than the mean *o*-Ps lifetime.

The  $T_g$ s estimated from the PALS data are in agreement with those obtained from the PVT data (Part I) and are somewhat smaller than those from DSC (Table 1). The mean hole volume at  $T_g$ ,  $\nu_{hg}$ , varies between 97 and 115 ( $\pm 5$ )  $\text{ \AA}^3$  with a mean of 111  $\text{ \AA}^3$ . Shrithawapong et al. [25] have observed  $\nu_{hg}$  values increasing from  $\sim 70$  to  $\sim 140 \text{ \AA}^3$  when the  $T_g$  of the polymer increases from 200 to 400 K. Such an increase is not clearly detected in our copolymers. With increasing MA content the thermal expansivities  $e_{hg} = d\nu_h/dT$  ( $T < T_g$ ) and  $e_{hr} = d\nu_h/dT$  ( $T > T_g$ ) decrease from  $e_{hg} = 0.22 \text{ \AA}^3 \text{ K}^{-1}$  to  $e_{hg} = 0.11 \text{ \AA}^3 \text{ K}^{-1}$  in the glassy state and from  $e_{hr} = 1.02 \text{ \AA}^3 \text{ K}^{-1}$  to  $e_{hr} = 0.75 \text{ \AA}^3 \text{ K}^{-1}$  in the rubbery state.

#### 3.2. Relations between specific total and free volume and hole size

The number of holes per mass unit,  $N_h'$ , may be estimated from one of the following relations [26] (see also Refs. [22,25,27–34]),

$$V = V_{\text{occ}} + V_{f0} + N_h' \nu_h, \quad (2)$$

$$V_f = (hV) = V_{f0} + N_h' \nu_h, \quad (3)$$

here, the free volume is expressed by  $N_h' \nu_h$ , the term  $V_{f0}$  may count for a possible deviation of the mean hole volume  $\nu_h$  estimated from the *o*-Ps lifetime  $\tau_3$  from the true mean hole volume [30,33],  $\nu_h^{\text{true}}$ ,

$$\nu_h = \nu_h^{\text{PALS}} = \nu_h^{\text{true}} - \nu_{h0}, \quad (4)$$

$\nu_h = \nu_h^{\text{PALS}}$  may be smaller than  $\nu_h^{\text{true}}$  ( $\nu_{h0} > 0$ ) since the volume of stretched holes is underestimated by Eq. (1) [35–38]. It might also be larger than the true average of the hole size distribution ( $\nu_{h0} < 0$ ) because of a lower detection threshold [37] and a possible preference of larger holes [39, 40]. Both of these effects act in different directions and it is unclear which the dominant effect is. We assume that  $\nu_{h0}$  is constant and not affected by the value of  $\nu_h$  which means that  $N_h'$  is not affected either ( $V_{f0} = N_h' \nu_{h0}$ ). In principle, all the other values in Eqs. (2) and (3) may vary.

Fig. 2 shows the specific volume,  $V$ , and Fig. 3 the specific free volume  $V_f = hV$ , each plotted as a function of  $\nu_h$ . The straight lines are due to linear fits of Eqs. (2) and (3) to the data in the temperature range of  $T > T_g$ . One observes that both  $V$  and  $V_f$  follow linear functions above  $T_g$  with slopes that show little variation as a function of the

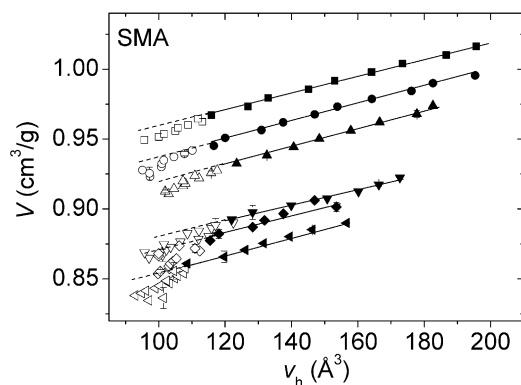


Fig. 2. Specific volume,  $V$ , vs. mean hole volume,  $\nu_h$ , for SMA copolymers. Symbols as in Fig. 1, filled, above  $T_g$ ; empty, below  $T_g$ .

composition of the SMA copolymer. The  $V_f$  data follow almost the same linear functions below  $T_g$  as above (Fig. 3). From this we may conclude that the hole number per mass unit,  $N_h'$ , is constant throughout the entire range of temperatures: it is independent of the temperature in the rubbery state and freezes in below  $T_g$ . The intersection of the fitted straight line with the y-axis,  $V_{f0}$ , is almost zero. We may conclude from this that the hole volume,  $\nu_h$ , calculated from  $\tau_3$  is a true representation of the mean hole size.

We note that in the case of the specific volume curves (Fig. 2) the values below  $T_g$  are always lower than predicted by extrapolation of the lines obtained from a linear fit above  $T_g$ . This deviation is due to the abrupt decrease in the coefficient of thermal expansion of the occupied volume at  $T_g$ . These results confirm this surprising effect, which was observed in the analysis of PVT data with S–S eos and discussed in detail in part I [1].

Linear  $V$  vs.  $\nu_h$  plots are typically observed in the literature above  $T_g$  and it is conventionally concluded from this that  $V_{occ}$  and  $N_h'$  are not functions of the temperature [25,32]. This conclusion is, however, not cogent. A linear behavior from which the constancy of  $N_h'$  can be concluded appears also if both  $V_{occ}$  and  $\nu_h$  vary linearly with the

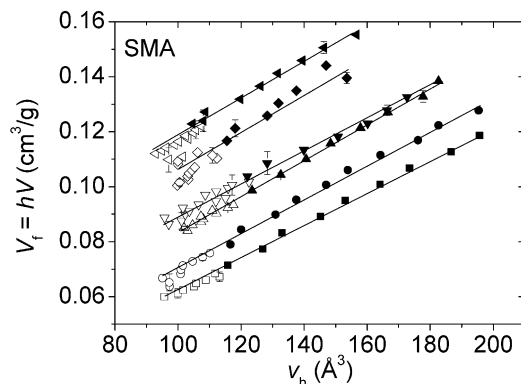


Fig. 3. Specific free volume,  $V_f$ , vs. mean hole volume,  $\nu_h$ , for SMA copolymers. Symbols as in Fig. 1, filled, above  $T_g$ ; empty, below  $T_g$ . Plots are shifted with increasing amount of MA away from PS to aid clear viewing, i.e. MA12 = +0.01 cm<sup>3</sup> g<sup>-1</sup>, MA35 = +0.05 cm<sup>3</sup> g<sup>-1</sup>.

temperature  $T$ . Assuming this, one may estimate  $N_h'$  from the following equations obtained by differentiation of Eq. (2) and assuming a constant  $N_h'$ :

$$N_h' = dV/d\nu_h - dV_{occ}/d\nu_h = (E_r - E_{occ,r})/e_{hr}, \quad (5)$$

or of Eq. (3)

$$N_h' = dV_f/d\nu_h = E_{fr}/e_{hr}, \quad (6)$$

where  $E_r = dV/dT$ ,  $E_{occ,r} = dV_{occ}/dT$  and  $E_{fr} = dV_f/dT$ , all at  $T > T_g$ , are the expansivities of the total, occupied and free specific volume above  $T_g$ . As Table 1 shows, the values of  $dV/d\nu_h$  are slightly larger than  $dV_f/d\nu_h$  ( $T > T_g$ ). This shows that for  $T > T_g$  the effect of thermal expansion of the occupied volume on the estimation of  $N_h'$  is small,  $E_{occ,r} \ll E_r$ . For PS we estimated a value of  $N_{hg}' = (0.60 \pm 0.04) \times 10^{21} \text{ g}^{-1}$  which may be compared with the literature values of 0.62 [28] and 0.8 [32] given in the same units. We can use the hole numbers per mass unit and the specific volume of the polymer to give the corresponding volume related hole number density,  $N_h(T) = N_h'/V(T)$ . These values calculated for  $T_g$  vary between  $N_h(T_g) = N_{hg} = 0.62$  and  $0.82 \text{ nm}^{-3}$  (Table 1).

The constancy of the hole density,  $N_h'$ , is an interesting result and confirms similar conclusions from other authors [25–33]. It means that all of the segmental motion above  $T_g$ , which can be pictured as the re-arrangement, creation and destruction of free volume holes, is mirrored in the mean size (and size distribution) of the holes but not their mean number density. This is revealed in experiments where properties that depend on polymer dynamics such as viscosity [41] and the diffusion of small guest molecules (gases [42,43] and ions [44,45]) are measured and show a clear relationship to the hole size detected by PALS.

At this point, we would like to draw the reader's attention to the following problem. In Eqs. (5) and (6), we have assumed, as has been done previously [26,33,34], that the mass-related hole density is independent of temperature. This seems reasonable to us, since the mass is temperature invariant. In the literature the hole fraction,  $h$ , from the S–S eos analysis is frequently plotted vs. the hole volume [27–30]. From the linearity of these plots the constancy of the volume related number density of holes,  $N_h$ ,  $h = N_h\nu_h$ , has been concluded. We have found that a plot of  $h$  vs.  $\nu_h$  cannot resolve this question except for the observation that the y-axis is crossed at a value further from zero than in the  $V_f$  vs.  $\nu_h$  plot,  $h_0 = 0.01$  compared with  $V_{f0} = 0.002$  (Table 1) for PS. The following way of comparing  $h$  with  $\nu_h$ , which was used previously for estimating the hole number [28,30] seems useful to answer this question. In a plot of  $h$  vs. temperature, the experimental data of the hole fraction  $h$  are fitted by the relation  $h(T) = B\nu_h(T)$  where  $B$  is a fitting constant. We have determined  $B = 0.58 \text{ nm}^{-3}$  by minimization of the variance of the fit over the whole range of temperatures. As Fig. 4 shows there are systematic deviations of the fitted curve from the experiments which

were also observed by Schmidt and Maurer [30] for poly(methyl methacrylate). The fitted curve has a larger slope than the experimental data. We observed that the excess slope corresponds just to the temperature dependence of  $V$ . When multiplying  $h(T)=B\nu_h(T)$  with  $V(T)$  one obtains  $V_f(T)=h(T)V(T)=(BV)\nu_h=B'\nu_h(T)$ . A fit of the specific free volume data  $V_f$  vs.  $\nu_h$  delivers  $B'=0.60\times 10^{21}\text{ g}^{-1}$  and a variance of the fit five times better than in the former case. As can be observed in Fig. 4 the systematic deviation of the fitted data from experiments has disappeared. This shows that the mass-related hole density ( $N_h'=B'$ ) is independent of temperature.

### 3.3. Local free volume distribution

Next, we compare the hole volume distribution calculated from the distribution of the  $o$ -Ps lifetime with the theory of thermal fluctuation [46,47]. We define the root-mean-square fluctuation in the fractional free volume by

$$\delta f_{\text{rms}} = (\langle \delta V_f^2 \rangle / \langle V \rangle^2)^{1/2}, \quad (7)$$

where  $\langle \delta V_f^2 \rangle = \langle (V_f - \langle V_f \rangle)^2 \rangle$  is the variance of the specific free volume fluctuation. Assuming that the thermal fluctuations in the hole density  $N_h'$  can be neglected in comparison with  $\nu_h$ , then  $\delta f_{\text{rms}}$  can be expressed by

$$\delta f_{\text{rms}} = (\langle N_h' \rangle / \langle V \rangle) \langle \delta \nu_h^2 \rangle^{1/2} = \langle N_h \rangle \langle \delta \nu_h^2 \rangle^{1/2}, \quad (8)$$

where  $\langle \delta \nu_h^2 \rangle = \langle (\nu_h - \langle \nu_h \rangle)^2 \rangle$ , the variance of the hole size distribution, we have calculated as the second moment of the number weighted hole size distribution,  $g_n(\nu_h)$ .  $g_n(\nu_h)$  is given by  $g_n(\nu_h) = g(\nu_h)/\nu_h$  and the volume weighted hole size distribution,  $g(\nu_h)$ , is calculated from the hole radius distribution,  $n(r_h)$ , via  $g(\nu_h) = n(r_h)/4\pi r_h^2$ .  $n(r_h)$  follows from the  $o$ -Ps annihilation rate distribution,  $\alpha(\lambda)$ , assumed in LT9.0 to be a log normal function,  $n(r_h) = -\alpha(\lambda)d\lambda_3/dr_h$  (see Refs. [19,20]).

We have plotted the PALS-measured values of  $\delta f_{\text{rms}}$  as a

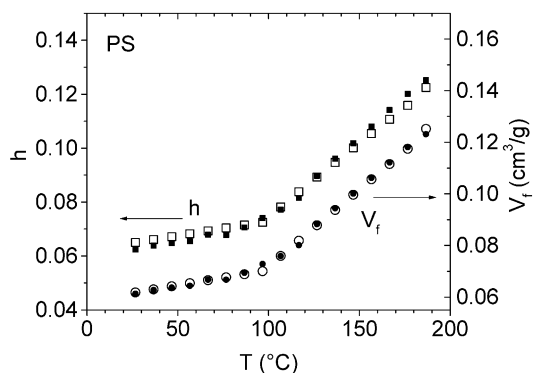


Fig. 4. The hole free volume fraction  $h$  and the specific free volume  $V_f=hV$  derived from PVT experiments with the S–S eos (empty symbols) in comparison with PALS data (filled symbols) obtained by fitting  $N_h\nu_h$  to  $h$  and  $N_h'\nu_h$  to  $V_f$  assuming either a constant volume related hole density,  $N_h$  ( $h=N_h\nu_h$ , squares), or a constant mass related hole density  $N_h'$  ( $V_f=N_h'\nu_h$ , circles).

function of temperature for PS in Fig. 5. The value of  $\sigma_{\nu_h} = \delta \nu_{h,\text{rms}} = (\langle \delta \nu_h^2 \rangle)^{0.5}$  increases almost linearly in PS from  $30 \text{ \AA}^3$  at room temperature to  $35 \text{ \AA}^3$  at  $T_g$  and further to  $70 \text{ \AA}^3$  at 473 K. Similar values are observed for the SMA copolymers. We found no systematic variation of  $\delta \nu_{h,\text{rms}}$  as a function of the copolymer composition. As can be seen in Fig. 5,  $\delta f_{\text{rms}}$  shows typical glass transition behaviour. Although the scatter is large, one observes a flat increase below  $T_g$ , and a stronger one above. As mentioned previously, in thermal equilibrium the spatial fluctuations of the free volume are identical with the time fluctuation. PALS detects these fluctuations provided that the relaxation times for segmental motion are larger than the  $o$ -Ps lifetime of 2–3 ns. Below  $T_g$  most of the fluctuations are ‘frozen-in’ and quasi-static.

Following conventional thermodynamics [46,47] the mean square fluctuation of the volume  $V$  about its mean value  $\langle V \rangle$  at equilibrium is related to the second derivative of the Helmholtz free energy  $F$  via  $\langle \delta V^2 \rangle = -k_B T / (d^2 F / dV^2)_{(V)}$ . With  $(d^2 F / dV^2)_{(V)} = -(dP/dV)_{(V)}$  and assuming that the fluctuation in the free and occupied volume are independent,  $\langle \delta V^2 \rangle = \langle \delta V_f^2 \rangle + \langle \delta V_{\text{occ}}^2 \rangle$ , one obtains for the root-mean-square fluctuation in the fractional free volume

$$\delta f_{\text{rms}} = (k_B T \kappa_f \langle V_f \rangle / \langle V \rangle^2)^{1/2} = (k_B T \kappa_f^* / \langle V \rangle)^{1/2} \quad (9)$$

where  $\kappa_f = -[1/V_f][dV_f/dP]_T$  is the isothermal compressibility of the free volume and  $\kappa_f^*(T) = -[1/V][dV_f/dP]_T$  is the fractional compressibility of the free volume; these values were discussed in Part I [1].

Thermal fluctuations are considered in a sub-volume  $\langle V \rangle$  embedded in, and being in thermodynamic contact with, a much larger volume. While  $\langle \delta V_f^2 \rangle / \langle V \rangle$  is independent of the chosen sub-volume,  $\langle \delta V_f^2 \rangle$  is not and  $\langle V \rangle$  must be chosen as the volume in which the fluctuations are desired. Robertson [46] considered this question as follows. For vinyl-type polymers, a chain segment of roughly four backbone carbon atoms, or two monomer units, plus 12 nearest neighbours of like size is expected to constitute a segmental rearrangement

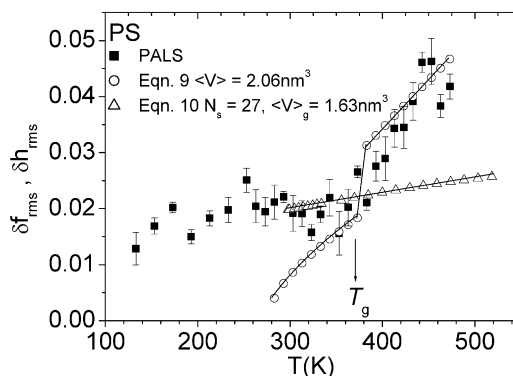


Fig. 5. Distribution of free volume as determined by PALS and Eq. 8 (filled squares), thermodynamic fluctuation theory (Eq. 9, open circles) and Robertson’s modification of S–S theory (Eq. 10, open triangles) for PS.



cell. This would yield 26 chemical repeating units, which occupy at  $T_g$  a volume of  $4.3 \text{ nm}^3$ .

We point out that the subvolume  $\langle V \rangle$  in Eq. (9) and the concept of a co-operative rearranging region (CRR) from theories of dynamic heterogeneity of glass forming liquids share similar characteristics, with the latter having been estimated, by time modulated- and conventional- differential scanning calorimetry, to have a size of  $1\text{--}10 \text{ nm}^3$  [48,49] at  $T_g$ . Domains of similar size were detected in nuclear magnetic resonance experiments by Spiess and collaborators [50]. Possibly, the hole detected by *o*-Ps may be considered as the inner part of the CRR (the Glarum–Levey defect [49]), and the volume of material containing one hole,  $1/N_h$ , can be identified with a CRR.

If one plots  $\delta f_{\text{rms}}^2$ , as defined by PALS experiments via Eq. (8), against  $(k_B T \kappa_f^*)$  then, according to Eq. (9), the gradient will be equal to  $1/\langle V \rangle$ . The fitting is only performed above  $T_g$  as Eq. (9) is derived assuming equilibrium. For PS the fits delivered a value of  $\langle V \rangle = 2.06 (\pm 0.2) \text{ nm}^3$  which is equivalent to 12 chemical repeat units. We found similar values for the SMA copolymers. This value is quite close to  $1/N_{\text{hg}} = 1.6 \text{ nm}^3$ .

The calculations from Eq. (9), as shown in Fig. 5 show a clear step in  $\delta f_{\text{rms}}$  at  $T_g$  to distinctly lower values and a further decrease with decreasing temperature which differs from the behaviour observed by PALS. This step is due to the step in the compressibility (see Part I [1]). A similar effect was observed when comparing electron density fluctuations studied by small angle X-ray scattering with this theory [51,52]. The reason for the deviation between  $\delta f_{\text{rms}}$  as determined from PALS and Eq. (9) is that the latter only describes the dynamic contribution to the disorder whereas PALS detects both dynamic and static contributions, with a quasi-static, or ‘frozen-in’, disorder clearly being important below  $T_g$ .

In the next step, we follow Robertson [46], who used the relation  $\langle \delta h^2 \rangle = -k_B T / (d^2 F / dy^2)_{(y)}$  together with the Helmholtz free energy  $F$  as given in the S–S eos,  $F = F(V, T, y)$ , to calculate the fluctuation in the fractional free volume (or hole fraction),  $h$ , to be

$$\langle \delta h^2 \rangle = \frac{1}{N_s} \times \left\{ \frac{1}{y^2} \left[ 1 + \frac{2}{y} \ln(1-y) + \frac{1}{1-y} \right] + \frac{1}{3} \frac{(2^{1/2} y \tilde{V})^{2/3} + (8/3) y (2^{1/2} y \tilde{V})^{1/3} + 3y^2}{y^2 (2^{1/2} y \tilde{V})^{1/3} - y} \right\}^{-1} + \frac{1}{3yT} [6.0066(y\tilde{V})^{-4} - 2.409(y\tilde{V})^{-2}] \quad (10)$$

Here,  $y = 1 - h$ ,  $\tilde{V} = V/V^*$  and  $\tilde{T} = T/T^*$  where  $V^*$  and  $T^*$  are the scaling volume and temperature. The theoretical background of these values and their determination from PVT experiments were discussed in detail in Part I [1]. As before, values of  $1/s = 0$  and  $s/3c = 1$  have been assumed (see Part I [1]).  $N_s (=Ns)$  is the number of lattice cells, defined according to the Simha–Somcynsky theory, in the sub-volume in which the fluctuations are desired. A

comparison of this model with PALS results has been done previously by Liu et al. [20]. Eq. (10) is derived under the general assumption of equilibrium, however, the specific assumption that the free energy is a minimum, has not been made. Therefore, Eq. (10) is expected to be valid not only above  $T_g$ , but also below, when being not too far from equilibrium [46]. If one assumes a fluctuation volume defined as  $\langle V \rangle = 1/N_h$  from the PALS data and then state that  $N_s = \langle V \rangle / \omega$ , where  $\omega (= 61 \text{ \AA}^3)$  is the volume of a lattice cell defined in Part I, a value of  $N_s = 27$  is reached.  $N_s$  can be interpreted as the cooperativity, that is the number of ‘particles’ i.e. cells per CRR as defined by Adam and Gibbs. The value of 27 reached here corresponds very well with estimates of 12–36 previously published by Beiner et al. [53] for a series of poly(alkyl methacrylates). These estimates were reached in the framework of a fluctuation approach to the glass transition introduced by Donth [49]. Fig. 5 shows that the variation of  $\delta h_{\text{rms}} = (\langle \delta h^2 \rangle)^{0.5}$  with temperature below  $T_g$  is similar to that measured by PALS. Above  $T_g$ , however, there is a marked difference which is consistent with the values calculated using Robertson’s method being unable to describe the sudden increase in dynamic contributions to the free volume distribution. We notice that the definition of  $\delta h = h - \langle h \rangle = V_f/V - \langle V_f \rangle / \langle V \rangle$  deviates from our definition of  $\delta f$ ,  $\delta f = V_f / \langle V \rangle - \langle V_f \rangle / \langle V \rangle$ , which leads to a damping in the increase of  $\delta h$ , but is not sufficient to explain the discrepancy to the PALS experiments.

Simha and Somcynsky’s theory describes a negligible variation of cell size whereas PALS detects a strong variation, particularly above  $T_g$ , in free volume hole size. Some authors attempt to overcome this by identifying the holes probed by *o*-Ps as a cluster of empty cells, described by the S–S theory, with varying numbers of cells  $i$  in each cluster. Vleeshouwers et al. [54] performed Monte Carlo simulations to obtain the cluster size distribution as a function of the hole fraction  $h(T)$ . The MC results were represented empirically by a decreasing exponential-like function describing the probability of a cell being in a cluster of  $i$  cells.

In calculating the cluster size distribution it is assumed that the probability of a cell being unoccupied is independent of the cells around it, and is, therefore, equal to the unoccupied fraction. This probability is the only input in calculating the cluster size distribution and it is, therefore, a purely statistical construct: the size of the cells is not required explicitly at this point and there are no material-specific inputs. In our analysis, we expect that the distribution in the cluster size will be affected by fluctuations in the fractional free volume and, therefore, attempt to account for this in the following way.

- We assume a Gaussian distribution of free volume fraction  $R(h, \langle \delta h^2 \rangle^{0.5})$  (normalised to have total area = 1) where  $h = \langle h \rangle$  calculated from the S–S eos (see paper I for

details [1]) and  $\langle \delta h^2 \rangle^{0.5}$  from Robertson's theory (see above).

- At each point,  $h$ , along this Gaussian distribution we calculate the Vleeshouwers cluster size distribution  $D(i, h)$ .
- We then calculate the volume fraction of each cluster size,  $i$ , which is equal to the probability,  $P(i)$ , of a given infinitesimal volume being part of a cluster of size  $i$ . For this we use the following equation:

$$P(i) = \sum_h \left[ \frac{R(h, \langle \delta h^2 \rangle^{0.5}) D(i, h)}{\sum_i D(i, h)} \right] \quad (11)$$

- The volume average cluster size is then calculated using Eq. (12).

$$\langle P_i \rangle = \frac{\sum_i i P(i)}{\sum_i P(i)} \quad (12)$$

- We then use  $P(i)$  to calculate the number average cluster size:

$$\langle N_i \rangle = \frac{\sum_i P(i)}{\sum_i \frac{P(i)}{i}} \quad (13)$$

Resulting plots of the two differing average cluster sizes against the mean hole size as measured by PALS were found to be fitted well by a straight line. The parameters of this straight line, however, depend on whether it is the volume,  $\langle P_i \rangle$ , or number,  $\langle N_i \rangle$ , average cell cluster size considered and these shall be dealt with separately. Intuitively, one might think that the number average cluster size is appropriate for comparisons with PALS results,  $\nu_h = \langle N_i \rangle \omega_i$ , where  $\omega_i$  can be calculated using this equation to be the size of the unoccupied lattice cells constituting the clusters, taken to be equivalent to the S–S cell size,  $\omega$ , calculated in part I [1]. When  $\nu_h$  is plotted against  $\langle N_i \rangle$ , however (Fig. 6 for PS), the straight line has a gradient varying between  $126 \text{ \AA}^3$  (PS) and  $90 \text{ \AA}^3$  (PS-co-MA(35%)) and a constant positive intercept with an average of 0.64 cells on the  $\langle N_i \rangle$ -axis, whereas a good fit of the above equation should go through the origin.

Alternatively, if the volume average cell size  $\langle P_i \rangle$  is taken then a plot of  $\nu_h$  vs.  $\langle P_i \rangle$  results in a straight line through the origin as shown in Fig. 6. This is consistent with a relationship of the type  $\nu_h = \langle P_i \rangle \omega_i$  where  $\omega_i$  is the size of a single cell which, for polystyrene, we find to be  $41 \text{ \AA}^3$ . The values for the other materials are shown in Fig. 7. These are of the same order of magnitude, but consistently lower than the cell volumes calculated directly using the characteristic scaling parameters, reported in part I [1] to be constant at  $61 \text{ \AA}^3$  for the entire series. One of the interesting aspects at

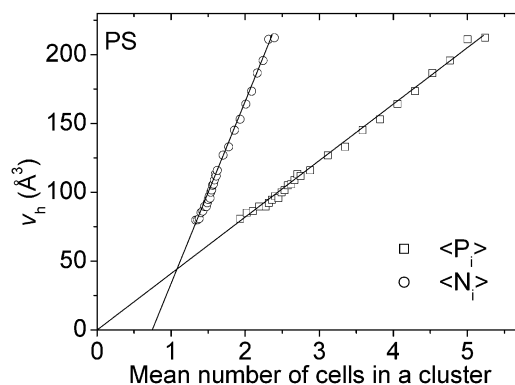


Fig. 6. Mean hole volume from PALS  $\nu_h$  vs. the mean number of cells per cluster, calculated following Vleeshouwers's method for PS. Squares,  $\langle P_i \rangle$ =volume average (Eq. 12). Circles,  $\langle N_i \rangle$ =number average (Eq. 13).

this juncture is the fact that in calculating the mean cluster size it is the volume- and not number-average cluster size which results in a fit passing through the origin and, therefore, supports the principle of clusters of S–S cells being sampled by positrons. One possible conclusion to be drawn from this is that the positrons sample free volume in a similar volume- and not number-average manner. A similar conclusion has been suggested by some of us in a previous paper [55].

#### 4. Conclusions

The free volume, as determined by PALS and PVT experiments, gets less as the MA content increases in a series of SMA random copolymers. For the hole size, measured by PALS this is particularly pronounced above  $T_g$ , where there is also a decrease in hole size expansivity with increasing MA content:  $1.02\text{--}0.75 \text{ \AA}^3 \text{ K}^{-1}$  ( $\pm 0.06$ ) as MA content increases from 0 to 35%. This is indicative of the rigid MA monomeric units stiffening the polymer chains, an effect which is also seen in the increase of  $T_g$  from 372 (0% MA) to 437 K (35% MA). The number of holes per unit

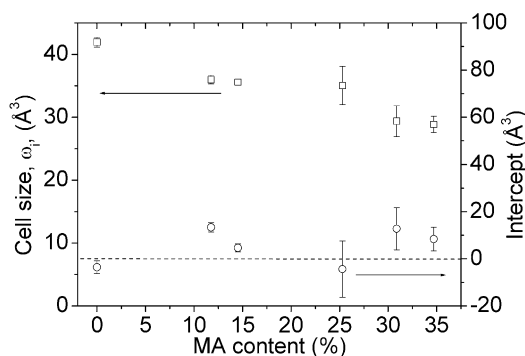


Fig. 7. Cell size,  $\omega_i$ , as determined by Vleeshouwers theory, and intercept of a plot of mean hole volume vs. mean number of cells per cluster,  $\langle P_i \rangle$ , (see Fig. 6), as a function of MA content for the full series of SMA copolymers.

mass is found to vary between 0.60 and 0.70 ( $\pm 0.04$ ) $\times 10^{21}$  g<sup>-1</sup> and be constant with temperature above  $T_g$ , this corresponds to a volume density of between 0.62 and 0.82 ( $\pm 0.04$ ) nm<sup>-3</sup>. The width of the free volume distribution compares favourably with fluctuations in free volume due to thermal effects and leads to a typical volume of 2.06 nm<sup>3</sup> within which these fluctuations take place. This is similar to the volume of a CRR. Clusters of unoccupied S–S cells at  $T_g$  are found to consist of typically 1.6 and 2.9 cells, taking the number and volume average, respectively. By comparing the sizes of the clusters with mean hole volumes from PALS data further evidence has been discovered that the positrons may sample holes in a volume average- and not number average-way.

## References

- [1] Part I, Kilburn D, Dlubek G, Pionteck J, Bamford D, Alam MA. *Polymer* 2005, this issue.
- [2] Dupasquier A, Mills Jr AT, editors. *Positron spectroscopy of solids*. Proc Int School Enrico Fermi, July 1993, Varenna, Italy. Amsterdam: IOS Press; 1993.
- [3] Mogensen OE. *Positron annihilation in chemistry*. Berlin: Springer; 1995.
- [4] Jean YC, Mallon PE, Schrader DM, editors. *Principles and application of positron and positronium chemistry*. Singapore: World Scientific; 2003.
- [5] (a) Jean YC. *Microchem J* 1990;42:72.  
(b) He YJ, Cao BS, Jean YC, editors. *Proceedings of the 10th international conference on positron annihilation*. Mater Sci Forum, 175–178, 1995, p. 59.
- [6] Pethrick RA. *Prog Polym Sci* 1997;22:1.
- [7] Ito Y, Suzuki T, Kobayashi Y, editors. *Proceedings of the 6th international workshop on positron and positronium chemistry (PPC.6)*, 7–11 June 1999, Tsukuba, Japan. *Radiat Phys Chem*, 58, 2000, p. 401 [no. 5–6].
- [8] Zoller P, Walsh CJ. *Standard pressure–volume–temperature data for polymers*. Lancaster, Basel: Technomic Publishing Co; 1995.
- [9] Simha R, Somcynsky T. *Macromolecules* 1969;2(4):342.
- [10] Utracki LA, Simha R. *Macromol Theory Simul* 2001;10:17.
- [11] Kansy J. *Nucl Instrum Methods A* 1996;374:235.
- [12] Kansy J. *LT for Windows*, Version 9.0, March 2002, PL-40-007 Katowice: Inst of Phys Chem of Metals, Silesian University, Bankowa 12, Poland, private communication.
- [13] Pionteck J, Reid V, MacKnight WJ. *Acta Polym* 1995;46:156.
- [14] Baugher AH, Kossler WJ, Petzinger KG, Pater RH. *Mater Sci Forum* 1997;57:255.
- [15] Hirata K, Kobayashi Y, Ujihira Y. *J Chem Soc, Faraday Trans* 1997; 93:139.
- [16] Tao SJ. *J Chem Phys* 1972;56:5499.
- [17] Eldrup M, Lightbody D, Sherwood JN. *Chem Phys* 1981;63:51.
- [18] Nakahishi N, Jean YC. In: Schrader DM, Jean YC, editors. *Positron and positronium chemistry, studies in physical and theoretical chemistry* 57. Amsterdam: Elsevier; 1988. p. 159.
- [19] Gregory RB. *J Appl Phys* 1991;70:4665.
- [20] Liu J, Deng Q, Jean YC. *Macromolecules* 1993;26:7149.
- [21] Schmidt M, Maurer FHJ. *Rad Phys Chem* 2000;58:535.
- [22] Schmidt M, Olsson M, Maurer FHJ. *J Chem Phys* 2000;112:11095.
- [23] Wang DL, Hirade T, Maurer FHJ, Eldrup M, Petersen NJ. *J Chem Phys* 1998;108:4656.
- [24] Hirade T, Maurer FHJ, Eldrup M. *Rad Phys Chem* 2000;58:465.
- [25] Srithawatpong R, Peng ZL, Olson BG, Jamieson AM, Simha R, McGervey JD, Maier TR, Halasa AF, Ishida H. *J Polym Sci, B: Polym Phys* 1999;37:2754.
- [26] Dlubek G, Stejny J, Alam MA. *Macromolecules* 1998;31:4574.
- [27] Kobayashi Y, Zehng W, Meyer EF, McGervey JD, Jamison S, Simha R. *Macromolecules* 1989;22:2302.
- [28] Yu Z, Yashi U, McGervey JD, Jamieson AM, Simha R. *J Polym Sci, B: Polym Phys* 1994;32:2637.
- [29] Schmidt M, Maurer FHJ. *Macromolecules* 2000;33:3879.
- [30] Schmidt M, Maurer FHJ. *Polymer* 2000;41:8419.
- [31] Hagiwara K, Ougizawa T, Inoue T, Horata K, Kobayashi Y. *Rad Phys Chem* 2000;58:525.
- [32] Bohlen J, Kirchheim R. *Macromolecules* 2001;34:4210.
- [33] Dlubek G, Bondarenko V, Pionteck J, Supey M, Wutzler A, Krause-Rehberg R. *Polymer* 2003;44:1921.
- [34] Dlubek G, Supej M, Bondarenko V, Pionteck J, Pompe G, Krause-Rehberg R, Emri I. *J Polym Sci, B: Polym Phys* 2003;41:3077.
- [35] Schmitz H, Müller-Plathe F. *J Chem Phys* 2000;112:1040.
- [36] Jean YC, Shi H, Dai GH, Huang CM, Liu L. *Mater Sci Forum* 1995; 175–178:691.
- [37] Jasinska B, Kozioł AE, Goworek T. *Acta Phys Pol A* 1999;95:557.
- [38] Jasinska B, Kozioł AE, Goworek T. *J Radioanal Nucl Chem* 1996; 210:617.
- [39] Ito Y. *Mater Sci Forum* 1995;175–178:627.
- [40] Süvegh K, Klapper M, Domján A, Mullins S, Vértes A. *Rad Phys Chem* 2000;58:539.
- [41] Bartoš J, Křištiak J, Šauša O, Bandžuch P, Zrubcová J. *Macromol Symp* 2000;158:111.
- [42] Okamoto K, Tanaka K, Katsube M, Kita H, Sueoka O, Ito Y. *Polym J* 1993;223:275.
- [43] Nagel C, Günther-Schade K, Fritsch D, Strunskus T, Faupel F. *Macromolecules* 2002;35:2071.
- [44] Bamford D, Dlubek G, Reiche A, Alam MA, Meyer W, Galvosas P, Rittig F. *J Chem Phys* 2001;115:7269.
- [45] Bamford D, Reiche A, Dlubek G, Alloin F, Sanchez JY, Alam MA. *J Chem Phys* 2003;118:9420.
- [46] Robertson RE. Free-volume theory and its application to polymer relaxation in the glassy state. In: Bicerano J, editor. *Computational modeling of polymers*. Midland, MI: Marcel Dekker; 1992. p. 297.
- [47] Waldram JR. *The theory of thermodynamics*. Cambridge: Cambridge University Press; 1985.
- [48] Götz W, Sjörgen L. *Rep Prog Phys* 1992;55:241.
- [49] Donth E. *The glass transition: relaxation dynamics in liquids and disordered materials*. Berlin: Springer; 2001.
- [50] Tracht U, Wilhelm M, Heuer A, Feng H, Schmidt-Tohr K, Spiess HW. *Phys Rev Lett* 1998;81:272.
- [51] Wendorff JH, Fischer EW. *Kolloid-Z Z Polym* 1973;251:876.
- [52] Wiegand W, Ruland W. *Prog Colloid Polym Sci* 1979;66:355.
- [53] Beiner M. *Macromol Rapid Commun* 2001;22:869.
- [54] Vleeshouwers S, Kluin JE, McGervey JD, Jamieson AM, Simha R. *J Polym Sci, B: Polym Phys* 1992;30:1429.
- [55] Dlubek G, Sen Gupta A, Pionteck J, Krause-Rehberg R. *Macromolecules* 2004;37:6606.